Int. J. of Sustainable Water & Environmental Systems
Volume 8, No. 2 (2016) 41-45

Estimation of Bacterial Growth Parameters Depicting Groundwater Bioremediation Using Inverse Modeling Moments

Mohamed M. Mohamed*

Civil and Environmental Engineering Department, United Arab Emirates University, P.O. Box 15551, Al-Ain, UAE.

Abstract

Spatial moments of contaminant plumes are tied to the distribution of bacterial populations through the biological term that appears in the transport equation. Theoretically, once spatial moments of both distributions are available, it is possible to estimate biological parameters such as the microbial maximum growth rate (μ_{max}), the contaminant half saturation coefficient (Ks), and the contaminant yield coefficient (Ys). New simple scaling relations between spatial moments of a contaminant plume and a bacterial population are developed and tested. Population of one microbial species is assumed to consume two solutes (an electron donor and an electron acceptor). A finite element model is used to test these relations through several testing problems. Results indicate the validity of such relations especially when the time interval between spatial moments decreases.

Keywords: *Groundwater, Scaling Relations, Moment Analysis, Biodegradation, Biological Parameters*

1. Introduction

A major concern in groundwater modeling is the effect of imposing small-scale determined parameters upon field scale transport problems. These parameters, which control the contaminant fate and transport in groundwater aquifers, can be separated into three groups, namely, physical, chemical, and biological parameters. Variability in any of these parameters could alter the behavior of a contaminant plume. Several researchers have focused on the non-reactive solutes and variability in hydraulic conductivity [e.g. 1, 2, 3, 4]. While other researchers emphasized reactive solutes and variability in aquifer chemical properties [e.g. 5, 6, 7, 8]. Other work [e.g. 9, 10, 11, 12, 13] showed that adsorption parameters might exhibit spatial variability.

Moment analysis methods had been proven to be useful tools in simplifying the transport-reaction equations. Such simplifications can lead to the estimation of spatial or temporal moments instead of concentrations. Goltz and Roberts [14], Cunningham et al. [15], Valocchi [16, 17], Espinoza and Valocchi [18], and Hu et al [19] used this technique to study the effect of different processes on solutes transport. Spatial moments' analysis was also used to study the behavior of reactive solutes going through advection, dispersion, and linear kinetic adsorption in heterogeneous aquifers [e.g. 7, 18, 20, 21, 22, 23]. Temporal moment expressions were developed for a conservative tracer pulse released simultaneously into *N* stream tubes with arbitrarily different advective–dispersive transport and steady flow speeds [24].

In this paper, spatial moment analysis is used to develop scaling relations tying the distribution of both the contaminant plume and bacterial distribution in groundwater aquifers. Such relations can be used to estimate the biological parameters (Y_S, K_S, and μ_{max}) that control contaminant fate, transport, and degradation. Scaling relations are developed in this paper. A microbial species is assumed to consume two solutes. Several testing problems are used to test the accuracy of the developed relations by employing the following steps. First, a finite element transport model [25] is used to simulate all testing problems and obtain contaminant and microbial concentration distributions at specific times. For each testing problem, moments of the contaminant and bacterial distributions are then calculated at the same times. Then, the developed scaling relations are employed to obtain values of the biological parameters (Y_S, K_S, and μ_{max}). Errors in estimating these parameters, by comparing the obtained values using scaling

* Corresponding author
Email: m.mohamed@uaeu.ac.ae

DOI: 10.5383/swes.8.02.002

relations to those originally assumed as input data for the transport model simulations, are then calculated. The behavior of these errors with the change of time interval is then studied for the different testing problems.

2. Moment Equations and Scaling Relations

Moment equations

For the simple case of one microbial species, a single electron donor, and a single electron acceptor:

$$\frac{\partial S}{\partial t} = -\frac{\partial}{\partial x_i}(J_s) - \frac{M}{Y_s}\mu \quad (1)$$

$$\frac{\partial A}{\partial t} = -\frac{\partial}{\partial x_i}(J_a) - \frac{M}{Y_a}\mu \quad (2)$$

$$\frac{dM}{dt} = \mu M - B M \quad (3)$$

where S and A are the aqueous phase concentration of the electron donor and electron acceptor, respectively, [$M_s L^{-3}$ or $M_a L^{-3}$]; J_s and J_a are the dissolved mass fluxes of the electron donor and electron acceptor, respectively,[$M_s L^{-2} T^{-1}$ or $M_a L^{-2} T^{-1}$] ; Y_s and Y_a (= 1/γ) are the yield coefficients.

In order to obtain the zeroth moment of the contaminant distribution, direct integration of equation 1 is performed as following:

$$\oint \frac{\partial S}{\partial t} dx_i = -\oint \frac{\partial}{\partial x_i}(J_s) dx_i - \oint \frac{M}{Y_s}\mu \, dx_i \quad (4)$$

where $\oint$ denotes integration over a control volume (CV) of the plume [e.g. x_i ={(-1,1),(-1,1)}i.e. {-1<x<1, -1<y<1}]. For a constant maximum growth rate μ_{max} and yield coefficient Y_s in the space, equation 4 can be written as:

$$\frac{\partial}{\partial t}\oint S dx_i = -\oint dJ_s - \frac{1}{Y_s}\oint M\mu \, dx_i \quad (5)$$

which can be rewritten as following:

$$\frac{\partial (m_{o-S}|_{CV})}{\partial t} = -(J_s|^{x_i^{max}} - J_s|^{x_i^{min}}) - \frac{1}{Y_s}\oint M\mu \, dx_i \quad (6)$$

where m_{o-S} is the zeroth absolute moment of electron donor S. Equation 6 can be then approximated to:

$$\frac{m_{o-S_2} - m_{o-S_1}}{t_2 - t_1} \cong -\frac{1}{2}\left((J_s|x_i^{max} - J_s|x_i^{min})|t_2 + (J_s|x_i^{max} - J_s|x_i^{min})|t_1\right) - \frac{1}{2Y_s}(\sum_{CV} M\mu \,|\, t_2 + \sum_{CV} M\mu \,|\, t_1)\Delta x \Delta y \quad (7)$$

where m_{o-S_2} *and* m_{o-S_1} are the zeroth absolute moment of the electron donor S at times t_2 and t_1, respectively. The smaller the time interval ($t_2 - t_1$), the more accurate equation 7 will be. Similar equation for the electron acceptor A can be written. Solution for equation 7 requires information about contaminant flux over the boundaries of the control volume. For the special case of infinite volume [xi ={(-∞,∞),(-∞,∞),(-∞,∞)}i.e. {-∞<x<∞, -∞<y<∞, -∞<z<∞}], assuming the following boundary conditions

$$J_s(x \rightarrow \pm\infty, t) = J_a(x \rightarrow \pm\infty, t) = 0 \quad (8)$$

Equation 7 can be rewritten as following:

$$\frac{m_{o-S_2} - m_{o-S_1}}{t_2 - t_1} \cong -\frac{1}{2Y_s}\left(\sum_R M\mu \Big|_{t_2} + \sum_R M\mu \Big|_{t_1}\right)\Delta x \Delta y \quad (9)$$

The zeroth absolute moment for the biomass distribution can be obtained by the direct integration of equation 3 as following:

$$\oint \frac{\partial M}{\partial t} dx_i = \oint (M\mu - BM) dx_i \quad (10)$$

assuming zero death rate equation 10 can be approximated to:

$$\frac{m_{o-M_2} - m_{o-M_1}}{t_2 - t_1} \cong \frac{1}{2}\left(\sum_{CV} M\mu \Big|_{t_2} + \sum_{CV} M\mu \Big|_{t_1}\right)\Delta x \Delta y \quad (11)$$

where m_{o-M_2} *and* m_{o-M_1} are the zeroth absolute moment of the biomass distribution at times t_2 and t_1, respectively. The first absolute moment for the biomass distribution can be obtained as following:

$$\oint \frac{\partial M}{\partial t} x dx_i = \oint (M\mu - BM) x dx_i \quad (12)$$

which can also be reduced to:

$$\frac{m_{1-M_2} - m_{1-M_1}}{t_2 - t_1} \cong \frac{1}{2}\left(\sum_{CV} M\mu X \Big|_{t_2} + \sum_{CV} M\mu X \Big|_{t_1}\right)\Delta x \Delta y \quad (13)$$

where m_{1-M_2} *and* m_{1-M_1} are the first absolute moment of the biomass distribution at times t_2 and t_1, respectively.

Scaling Relationships

In this section we illustrate how the moment equations obtained so far can be used to obtain values of the biological parameters. Dividing equation 11 by equation 7 yields:

$$Y_S \cong -\frac{m_{o-M_2} - m_{o-M_1}}{m_{o-S_2} - m_{o-S_1} + \Delta t \Delta J_s} \quad (14)$$

where $\Delta t = (t_2 - t_1)$ and ΔJ_s=

$$\frac{1}{2}\left((J_s|^{x_i^{max}} - J_s|^{x_i^{min}})\Big|_{t_2} + (J_s|^{x_i^{max}} - J_s|^{x_i^{min}})\Big|_{t_1}\right)$$

Similar equation to (Eqn. 14) can be written for the electron acceptor. For infinite domain, $\Delta J_s = \Delta J_a = 0$. On the other hand, dividing equation 13 by equation 7 yields

$$\frac{m_{1-M_2} - m_{1-M_1}}{m_{0-S_2} - m_{0-S_1} + \Delta t \Delta J_S} \cong -Y_S$$

$$\frac{\left(\sum_{CV} M\left(\frac{S}{K_S+S}\right)\left(\frac{A}{K_a+A}\right)X\Big|_{t_2} + \sum_{CV} M\left(\frac{S}{K_S+S}\right)\left(\frac{A}{K_a+A}\right)X\Big|_{t_1}\right)}{\left(\sum_{CV} M\left(\frac{S}{K_S+S}\right)\left(\frac{A}{K_a+A}\right)\Big|_{t_2} + \sum_{CV} M\left(\frac{S}{K_S+S}\right)\left(\frac{A}{K_a+A}\right)\Big|_{t_1}\right)} \quad (15)$$

Again for an infinite domain, one can put ΔJs = ΔJa = 0 in equation 15. Similar equation can also be written for the electron acceptor. Values of half saturation coefficients K_s and K_a can then be obtained by solving these two equations (equation 15 and the similar one for the electron acceptor). Using these values along with the previously obtained yield coefficients Y_s and Y_a, the maximum bacterial growth rate can then calculated using one of the equations 9, 11, or 13.

3. Testing Examples and Sensitivity Analysis

A two-dimensional *x*-*y* homogeneous aquifer with dimensions 50 m × 25 m (Figure 1) and a constant velocity in *x*-direction (V_x) of 0.5 m/d is assumed. The longitudinal and transverse dispersivities are chosen to be 0.1 and 0.05 m, respectively, while the porosity is assumed to be 0.3. An instantaneous discharge of 1 mg/l of contaminant at time t = 0 is released as an areal source of contamination with dimensions 5 m × 3 m (Figure 1). The centroid of this initial contaminant is located at (0, 0). The left and right boundaries are assigned constant head values to produce the constant velocity of 0.5 m/d, whereas the top and bottom boundaries are considered impervious. The aquifer domain is represented by a mesh of 31,250 rectangular elements (250 x 125) and 31,626 nodes. This example is pertained to examine the scaling relations obtained. Bacteria are assumed to have initial uniform distribution with concentration 0.01 mg/l. We show results only for contaminant parameters (electron donor); which are Y_s, K_s, and μ_{max}.

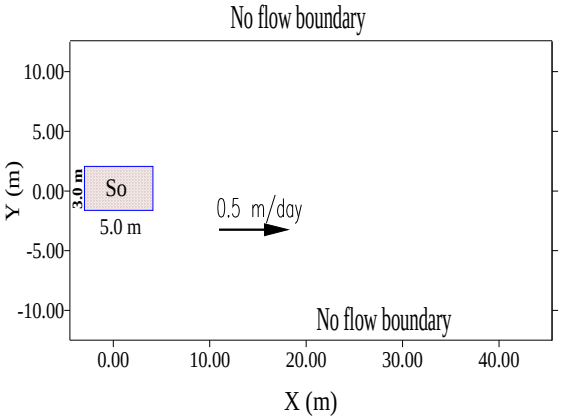

Figure 1. Problem Layout

Seven testing problems are employed to test the proposed relations. Biological input parameters for these problems are given in Table 1. The chosen values in this paper are close to those used by Schirmer et al. [26, 27]. Using the transport model, contaminant and biomass concentrations are obtained at each node every 5 days (t = 5, 10 ….70 days). Using these concentrations, the zeroth moment for both the contaminant and the biomass distributions and the first moment for the biomass distribution are then calculated at times (t = 5, 10 …70 days). Then, the scaling relations (Equations 11, 14, and 15) are used to estimate the biological parameters. First, Equation 14 is used to obtain values of contaminant yield coefficient Y_S. Equation 15 is used next to calculate values of the half saturation coefficient K_S. Finally, using equation 11, values of the bacterial maximum growth rate μ_{max} are attained. The biological parameters are obtained using all possible combinations of t_1 and t_2 (equations 11, 14, and 15). All obtained estimates of the biological parameters for all combinations of t_1 and t_2 are then separated into groups according to the interval between the used two time values ($\Delta t = t_2 - t_1$). The percentage errors (eP) in estimating each of the biological parameter are then calculated (equation 38). Subsequently, for each value of Δt, an average estimate (arithmetic mean) for the error (EP) in estimating each of the biological parameters (μ_{max}, K_s, or Y_s) is calculated (Equation 39). The minimum time interval was obviously 5 days, however, the maximum time interval was chosen to be 30 days in order to have sufficient values of the error to be averaged. This error represents the approximation in the differentiation and integration in the left and right hand sides of equation 14, respectively, to obtain equation 15. Looking carefully at these equations, it is expected that the error will be higher for greater values of Δt.

Table 1. Biological Input Parameters

	Y_S	K_S (mg/l)	μ_{max} (day^{-1})
Problem 1	0.01	5	0.5
Problem 2	0.05	5	0.5
Problem 3	0.1	5	0.5
Problem 4	0.01	5	1.0
Problem 5	0.01	5	2.0
Problem 6	0.01	3	0.5
Problem 7	0.01	7	0.5

For each value of Δt (5, 10, 15….30) and for any biological parameter P

$$eP = \frac{\left|P(t_1, t_1 + \Delta t) - OP\right|}{OP} x100 \quad ,$$

t_1=5, 10, 15, ... days

(16)

$$EP = \frac{\sum_{n=1}^{N} eP_n}{N} \quad (17)$$

where P (t_1, $t_1+\Delta t$) is the estimated value of the biological parameter P (Y_S, K_S, or μ_{max}) using moments scaling relationships obtained at t_1 and $t_2=t_1+\Delta t$, OP is the original value of P (input data, Table 1), eP is the error in estimating the

biological parameter P compared to OP, EP is the average percentage error of the biological parameter P (EY_S, EK_S, or $E\mu_{max}$) obtained for same time interval Δt, and N is the total number of values of P (or eP) obtained for the time interval Δt (N = 13, 12, ….. 8 for Δt = 5, 10, …..30 days, respectively).

Figure 2 represents the change in the estimated average error of the yield coefficient (EY_s) with the change in time interval. As can be seen from this figure, the error is stable (around 3%) for almost all seven testing problems, especially when time interval is small. Figure 2 also shows that increasing Y_s (problems 2 and 3) or increasing K_s (problem 7) causes EY_s to increase. Increasing μ_{max} (problem 5), on the other hand, causes the same error to decrease. This is probably because μ_{max} appears in the numerator of the biological term in the transport equation (Equation 9), while both Y_s and K_s appear in the denominator of the same equation.

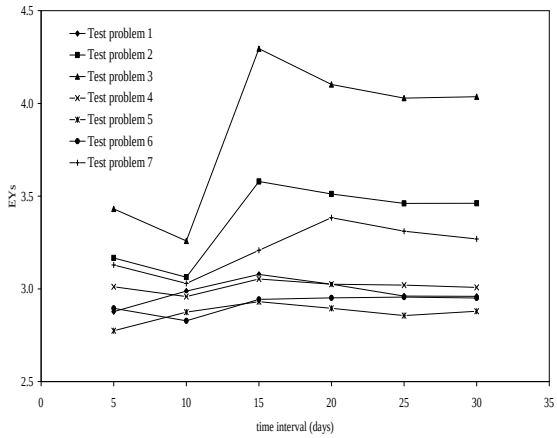

Figure 2. Change in the Average Percentage Error of YS with the Change in Time Interval

The change in the average error of K_s against time interval is given in Figure 2b. Generally, the error increases (almost linearly) with the increase in the time interval. However, the average error is ranging from 1% to 5% when the interval was 5 days and from 2% to 11% when the interval was 30 day. When the value of K_s is decreased from 5 mg/l (problem 1) to 3 mg/l (problem 6), EK_s increased at all intervals. This is consistent with the decrease in EK_s observed when K_s is increased to 7 mg/l in problem 7. Increasing Y_s, in problems 2 and 3, caused EK_s to increase compared to problem 1. Conversely, the increase in μ_{max} presented in problems 4 and 5 reduces EK_s at all values of Δt compared to problem 1 (Figure 3).

In Figure 4, the evolution of the average error in μ_{max} ($E\mu_{max}$) versus time interval is shown. This figure clearly shows that this error increases when μ_{max} is increased (problems 4 and 5) or K_s is decreased (problem 6). The same figure, however, demonstrates that $E\mu_{max}$ is decreased when Y_s is increased in problems 2 and 3. This observed behavior of $E\mu_{max}$ could be explained by comparing the total contaminant biodegraded mass of the seven problems. In general, the greater the biodegraded mass, the higher $E\mu_{max}$ is obtained. For example, problem 5 with the greatest simulated biodegraded mass (94%) presents the highest value of $E\mu_{max}$ at all intervals. Problem 3, on the other hand, which has the smallest biodegraded mass (9%), presents the lowest $E\mu_{max}$ (Figure 4).

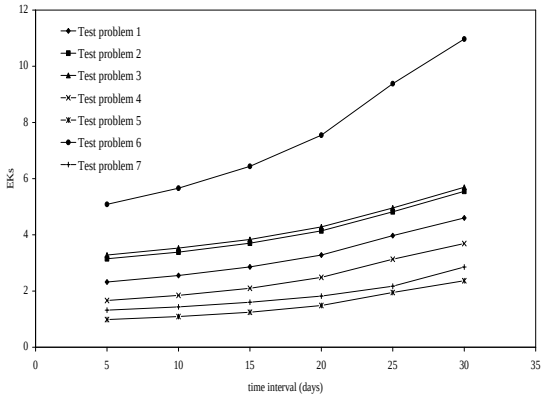

Figure 3. Change in the Average Percentage Error of K_S with the Change in Time Interval

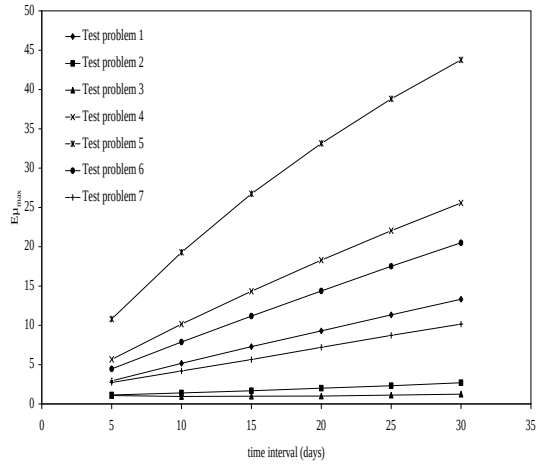

Figure 4. Change in the Average Percentage Error of «$_{max}$ with the Change in Time Interval

4. Summary and Conclusions

The errors in estimating the biological parameters are generally small for all simulated testing problems mainly because moments were calculated using concentrations at all nodes. Errors are generally increasing with the increase of the time interval. Increasing the yield coefficient (Y_s) causes the error in both Y_s and K_s to increase and the error in μ_{max} to decrease. On the other hand, increasing the half saturation coefficient K_s, only causes the error in Y_s to increase; while causes the error both K_s and μ_{max} to decrease. Finally, an increase in the maximum bacterial growth rate μ_{max} causes decrease in the estimated error of both Y_s and K_s and increase in the error of μ_{max}.

Acknowledgements

This research was partially funded by the NWC at UAEU (Grants numbers 31R008 and 31N166).

References

[1] Dagan G. Solute transport in heterogeneous porous formations. J. Fluid Mech.1984;145:151-177.

[2] Dagan G. Time-dependent macrodispersion for solute transport in anisotropic heter

[3] Gelhar LW and Axness CL. Three-dimensional stochastic analysis of macrodispersion in aquifers. Water Resour. Res. 1983;19:161-180.

[4] Gelhar LW, Gutjahar AL, and Naff RL. Stochastic analysis of macrodispersion in a stratified aquifer. Water Resour. Res. 1979;15:1487-1397.

[5] Metzger D, Kinzelbach H, and Kinzelbach W. Effective dispersion of a solute cloud in a chemically heterogeneous porous medium: Comparison of two ensemble-averaging procedures. Water Resour. Res. 1996;32:3311-3319.

[6] Miralles-Wilhelem, F and Gelhar LW. Stochastic analysis of sorption macro-kinetics in heterogeneous aquifers. Water Resour. Res. 1996;32:1541-1549.

[7] Schafer W, and Kinzelbach W. Numerical investigations into the effects of aquifer heterogeneity on in-situ bioremediation. In-Situ and On-Site Bioreclamation, Batelle Mem. Inst., Columbus, Ohio 1991:196–225.

[8] Tompson AFB, Schafer AL, and Smith RW. Impacts of physical and chemical heterogeneity on contaminant transport in a sandy porous media. Water Resour. Res. 1996;32:801-818.

[9] Barber Lb, Thurman EM, and Runnells DD. Geochemical heterogeneity in a sand and gravel aquifer: Effect of sediment mineralogy and particle size on the sorption of chlorobenzenes. J. Contam. Hydrol 1992;9(1/2):35-54.

[10] Davis LA, Fuller CC, Coston JA, Hess KM, and Dixon E. Spatial heterogeneity of geochemical and hydrologic parameters affecting metal transport in groundwater, Environmental Protection Agency, Washington, D.C., 1993.

[11] Mackay DM, Freyberg DL, Roberts PV, and Cherry JA. A natural gradient experiment on solute transport in a sand aquifer 1: Approach and overview of plume migration. Water Resour. Res. 1986;22:2017-2029.

[12] Robin MJL, Sudicky EA, Gillham RW, and Kachanoski RG. Spatial variability of strontium distribution coefficients and their correlation with hydraulic conductivity in the Canadian forces base borden aquifer. Water Resour. Res. 1991;27: 2619-2632.

[13] Mohamed, M., Hatfield K, Hassan AE, and Klammler H. Stochastic Evaluation of Subsurface Contaminant Discharges Under Physical, Chemical, and Biological Heterogeneities, Advances in Water Resources, Volume 33, Issue 7, 801-812, 2010a.

[14] Goltz, M, and Roberts P. Using the method of the moments to analyze three-dimensional diffusion-limited solute transport from temporal and spatial perspectives. Water Resour. Res. 1987;23:1575-1585.

[15] Cunningham JA, Goltz MN, and Roberts PV. Simplified expressions for spatial moments of groundwater contaminant plumes. Technical note. Journal of Hydrol. Eng. 1999;4:377-380.

[16] Valocchi AJ. Theoretical analysis of deviations from local equilibrium during sorbing solute transport through idealized stratified aquifer. J. Contam. Hydrol 1988;2:191-207.

[17] Valocchi AJ. Spatial moments analysis of the transport pf kinetically adsorbing solutes through stratified aquifers. Water Resour. Res. 1989;25:273-279.

[18] Espinoza C and Valocchi AJ. Temporal moments analysis of transport in chemically heterogeneous porous media. Journal of Hydrol. Eng 1998;3:276-284.

[19] Hu BX, Deng FW, and Cushman JH. Non-local reactive transport with physical and chemical heterogeneity: Linear nonequilibrium sorption with random K_d. Water Resour. Res. 1995;31:2239-2252.

[20] Dagan G, Cvetkovic VD, and Shapiro A. A solute flux approach to transport in heterogeneous formations 1: The general framework. Water Resour. Res. 1992; 28: 1369-1376.

[21] Dagan G and Cvetkovic VD. Spatial moments of a kinetically sorbing solute plume in a heterogeneous aquifer. Water Resour. Res. 1993; 29:4053-4061.

[22] Quinodoz H, and Valocchi A. Stochastic analysis of the transport of kinetically sorbing solutes in aquifers with randomly heterogeneous hydraulic conductivity. Water Resour. Res. 1993;29:3227-3240.

[23] Selroos J and Cvetkovic V. Mass flux statistics of kinetically sorbing solute in heterogeneous aquifers: Analytical solution and comparison with simulations. Water Resour. Res. 1994;30:63-69.

[24] Bardsley WE. Temporal moments of a tracer pulse in a perfectly parallel flow system. Advances in Water Res. 2003;26:599-607.

[25] Mohamed, M. and K. Hatfield. Dimensionless Monod parameters to summarize the influence of microbial inhibition on the attenuation of groundwater contaminants. Biodegradation, 22:877–896, 2011.

[26] Schirmer M, Molson JW, Frind EO, and Barker JF. Biodegradation modeling of a dissolved gasoline plume applying independent laboratory and field parameters. J. Contam. Hydrol. 2000; 46:339-374.

[27] Mohamed, M., N. Saleh, and M. Sherif. Modeling In-Situ Benzene Bioremediation in the Contaminated Liwa Aquifer Using the Slow-Release Oxygen Source Technique. Environmental Earth Sciences, 61(7), 1385-1399, 2010.